Hybrid Dynamic Neural Network and PID Control of Pneumatic Artificial Muscle Using the PSO Algorithm

Mahdi Chavoshian   Mostafa Taghizadeh   Mahmood Mazare

School of Mechanical Engineering, Sh. Beheshti University, Tehran 16589-53571, Iran

Abstract: Pneumatic artificial muscles (PAM) have been recently considered as a prominent challenge regarding pneumatic actuators specifically for rehabilitation and medical applications. Since accomplishing accurate control of the PAM is comparatively complicated due to time-varying behavior, elasticity and ambiguous characteristics, a high performance and efficient control approach should be adopted. Besides of the mentioned challenges, limited course length is another predicament with the PAM control. In this regard, this paper proposes a new hybrid dynamic neural network (DNN) and proportional integral derivative (PID) controller for the position of the PAM. In order to enhance the proficiency of the controller, the problem under study is designed in the form of an optimization trend. Considering the potential of particle swarm optimization, it has been applied to optimally tune the PID-DNN parameters. To verify the performance of the proposed controller, it has been implemented on a real-time system and compared to a conventional sliding mode controller. Simulation and experimental results show the effectiveness of the proposed controller in tracking the reference signals in the entire course of the PAM.

Keywords: Dynamic neural network (DNN) control, hybrid control, pneumatic muscle, particle swarm optimization, sliding mode control.

1 Introduction

Pneumatic artificial muscle (PAM) is a type of pneumatic actuator that has many advantages such as light weight, low mass to force ratio and inherent compliance. Due to mentioned benefits, the PAM has been utilized in various applications in the field of robotics and medical industry. Despite these characteristics, the dynamics of the flow and pressure as well as the time-varying behavior have increased the nonlinearity of the PAM, which play a crucial role in control of the pneumatic actuators. Extracting the dynamic model covering the entire course of the actuator is a key challenge in terms of modeling and control of the PAM.

Besides the above mentioned challenges, limited course length is another predicament with the PAM control. Maximum displacement of a PAM is about 25 percent of its initial length and that is why a couple of proposed models and control methods have ineffective performance. Thus, using the PAM in various applications leads to enlarging the device dimensions.

Consequently, to overcome the aforementioned drawbacks, many approaches have been employed by the researchers to control the pneumatic muscle. In some early research, the linear state space model around a fixed

equilibrium point has been considered[1, 2]. Owing to the nonlinear nature of the pneumatic muscle, these approaches have never introduced a high efficiency and accurate response. As a consequence, adaptive control approaches have been used in [3, 4]. The well-known proportional integral derivative (PID) control is also presented in the conventional studies for control of the pneumatic muscles[5, 6]. Krichle et al.[7] and Shen[8] developed the nonlinear model-based control for the PAM in a linear antagonistic joint. Krichle designed an observer for unmodeled force, and also a controller for position control with 2 mm accuracy. Furthermore, a sliding mode control was presented by Shen for controlling the position of the PAM through experimental evaluation with tracking accuracy of 1 mm for sinusoidal reference.

The artificial neural network (ANN) has been considered and applied as a strengthening strategy for modeling and control of the nonlinear and complex systems. When the number of variables in a problem are relatively high, using artificial intelligence methods can be beneficial for design optimization, parameter identification, and sensitivity analysis[9]. Due to its vigorous performance, a wide variety of ANN applications in modeling and control of the nonlinear systems have been reported. In order to enrich the performance of the neural networks, dynamic neural networks (DNN) are suggested in modeling of the nonlinear systems[10]. To dominate the disadvantages of the PAM, intelligent methods such as the neural network based model and controller are applied[11–13]. New hybrid adaptive feed-forward neural network and

PID controllers have been proposed to adjust the selective compliance assembly robot arm (SCARA) parallel robot position actuated by the PAM[14]. A hybrid PID and neural network controller[15, 16], hybrid neural-fuzzy controller[17, 18], self-organizing fuzzy controller[19] and nonlinear predictive control based on the echo state Gaussian process[20] have been applied to achieve a precise control of the PAM. Also, a neural network fuzzy sliding mode control is suggested in [21] to accurately control a 1-DOF manipulator with PAM actuator. In recent years, diverse stochastic based optimization techniques such as harmony search algorithm, genetic algorithm, ant colony, and particle swarm optimization (PSO) have been used to solve the miscellaneous optimizations. Moreover, PSO algorithms have given accurate solutions considering low time-consuming duration[22]. PSO has naturally followed the behavior of fish and bird schooling and is considered as a stochastic global optimization technique. Mazare et al.[23] proposed a hybrid DNN and PID controller for position control of a pulse width modulation (PWM)-driven pneumatic actuator in which controller parameters are optimized using a metaheuristic algorithm.

Hence, among the above research, the entire course which is a key challenge of the PAM has not been covered. It should be noted that in all of the above mentioned references except [8, 17], the pressure control valve is applied that not only creates a tremendous cost but also simplifies the governing equations. In addition, compared to previous works, longer course length has been covered in [24, 25] using the pressure control valve. The most important outcome of this research is to consider the whole displacement of the pneumatic muscle′s motion while under control, which is equivalent to 25% of the muscle′s initial length. The second one is the dimensions of the muscle and consequently the overall size of the robot which will be decreased if the length of controlled motion maximizes. Also in this research a proportional valve was used which has a lower price and makes the model complicated.

In this paper, a hybrid structure using DNN and PID controllers is proposed for position control of the PAM and then, in order to obtain controller parameters, integral time absolute error is selected as a cost function which is optimized via PSO algorithm. Compared to conventional methods, it can be expressed that ANN presents the better performance. It should be noted that the DNN has been trained by experimental data, which is gathered from an experimental setup to provide a realistic condition. In other words, to enhance training performance and minimize the tracking error, the factor of learning neurons has been optimized. Proposing a new hybrid controller, combining specific types of dynamic neural networks and PID which is optimized by PSO is the main contribution of the manuscript. Moreover, applying the controller for PAM systems with specific applications is another one. It is worth mentioning that the dynamic neural network is a most prominent choice compared to the static network. Well-suited input is provided regarding the PAM setup and considered as the experimental model input while the required data is attained for training the neural network. The number of neurons and layers are obtained according to the considered data set and by exploring the various structures of the networks in terms of appropriate delay of inputs and outputs. To eliminate available objectionable performance of the system, the extracted data has been filtered properly, which is practically adequate to be applied to the PAM setup. The effectiveness of the proposed controller is verified through simulating on the verified model in presence of disturbances and uncertainties and then, implementing on a real system.

The remainder of this paper is organized as follows. In Section 2, the mathematical model of the PAM is extracted and tested by experimental data. The architecture of a DNN is illustrated in Section 3. Section 4 is concerned with designing a hybrid DNN and PID controller. Simulation and experimental results are presented in Sections 5 and 6, respectively. This paper ends with some concluding remarks in Section 7.

2 Dynamic modeling

This section aims to extract the mathematical model of a vertically suited PAM that holds a mass. The most appropriate modeling method associated with this PAM was proposed by Chou and Hannaford[26]. They derived a mathematical relation between the force and displacement of the load based on the static equation of pneumatic muscle force.

$$F = \frac{\pi d_{90}^2 P}{4} \left(3\cos^2\theta - 1\right) \tag{1}$$

where F, P and θ are pneumatic muscle force, pressure, the angle of muscle threads, respectively, and also d_{90} is the minimum muscle diameter. Considering the effect of muscle membrane thickness, Chou and Hannaford have proposed an enhanced version of (1) as follows:

$$F = \frac{\pi d_{90}^2 P}{4} \left(3\cos^2\theta - 1\right) + \pi p \left[d_{90} t_k \left(2\sin\theta - \frac{1}{\sin\theta}\right) - t_k^2\right]. \tag{2}$$

However, this function is highly nonlinear and its application for a model-based method results in a highly complicated control. Therefore, a tradeoff between control difficulty and tracking precision is required.

Based on the Chou and Hannaford method, Shen[8] proposed a single input single output (SISO) model for pneumatic muscle in a linear antagonistic joint. The control signal of the valve and third derivative of the position are considered as input and output of the model, respectively. Incorporating the pressure dynamic and orifice equations into the proposed model make it more suit-

able for experimental tests. As can be seen in (1), the force is a function of the muscle thread's angle. However, he modifies this equation so as to govern a function of the force versus the position of the muscle end as follows:

$$F = \left\{ \frac{[3(L_0 - x)^2 - b^2]}{4\pi n^2} \right\} \times (P - P_{atm}) \qquad (3)$$

where x, L_0, b, n and P_{atm} are the position, muscle length, thread length, number of threads and environmental air pressure, respectively.

Fig. 1 shows the schematic of the system under study. The system model has been extended based on Chou-Hannaford's equation and Shen's method. For this system, the dynamic equation of the mass can be written as follows.

$$M\ddot{x} = F - Mg \qquad (4)$$

where g is gravitational term. Substituting (1) into (4) gives

$$\ddot{x} = \left\{ \frac{[3(L_0 - x)^2 - b^2]}{4M\pi n^2} \right\} \times (P - P_{atm}) - g. \qquad (5)$$

(a) Initial length muscle   (b) Pressurized muscle
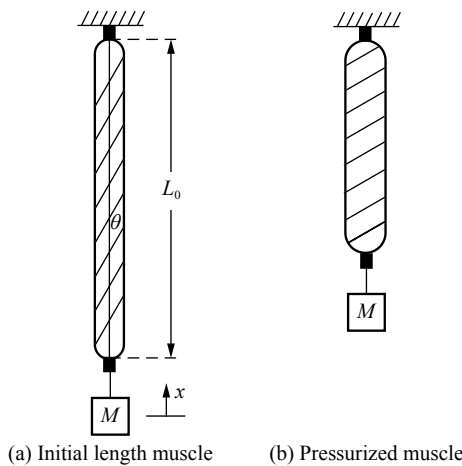
Fig. 1   Schematic structure of the experimental setup

If the pressure control valve is applied, the model will be simple and does not require further action and the model is complete. However, to enhance the precision of the model, a proportional valve has been used in this paper. Thus, taking a time-derivative of (5), the pressure dynamic is obtained as

$$\dddot{x} = \left\{ \frac{[3(L_0 - x)^2 - b^2]}{4M\pi n^2} \right\} \times \dot{P} - \frac{3[(L_0 - x)(P - P_{atm})]}{2M\pi n^2}\dot{x}. \qquad (6)$$

It can be seen that g disappears after derivation. Note

that for calculating the mass motion by integrating from $\ddot{x}$, the gravity acceleration must be added as an integration constant in simulation. Assuming the air as ideal gas, $\dot{P}$ is given by

$$\dot{P} = \frac{\gamma RT\dot{V}}{\dot{V}} - \frac{\gamma P}{V}\dot{V} \qquad (7)$$

where V, T, P and γ are the muscle volume, air temperature, universal constant of the gas and specific heat coefficient, respectively. Equations (8) and (9) have been proposed for muscle volume and its derivative in terms of time dependencies on the motion by Shen[8].

$$V = \frac{(L_0 - x)[b^2 - (L_0 - x)^2]}{4\pi n^2} \qquad (8)$$

$$\dot{V} = \frac{-b^2 + 3(L_0 - x)^2}{4\pi n^2}\dot{x}. \qquad (9)$$

Substituting (7)–(9) into (6) results in

$$\ddot{x} = \frac{C}{M}\dot{m} - \frac{K}{M}\dot{x} \qquad (10)$$

where C and K are determined to be

$$C = \frac{\gamma RT[3(L_0 - x)^2 - b^2]}{(L_0 - x)[b^2 - (L_0 - x)^2]} \qquad (11)$$

$$K = \frac{3[(L_0 - x)(p_b - p_{atm})]}{2\pi n^2} + \frac{\gamma[3(L_0 - x)^2 - b^2]^2 P}{4\pi n^2 (L_0 - x)[b^2 - (L_0 - x)^2]}. \qquad (12)$$

Also, $\dot{m}$ is the flow rate which can be obtained from the following orifice equations of the valve.

$$\psi(P_u, P_d) =$$
$$\begin{cases} \sqrt{\frac{\gamma}{RT}\left(\frac{2}{\gamma+1}\right)^{\frac{\gamma+1}{\gamma-1}}} C_f P_u, & \text{if} \quad \frac{P_d}{P_u} \leq C_r \\ \sqrt{\frac{2\gamma}{RT(\gamma-1)}}\sqrt{1 - \left(\frac{P_d}{P_u}\right)^{\frac{\gamma-1}{\gamma}}}\left(\frac{P_d}{P_u}\right)^{\frac{1}{\gamma}} C_f P_u, & \text{otherwise.} \end{cases}$$
$$(13)$$

In (13), for calculating ψ when the air is flowing into the muscle, we have $P_u = P_s$ and $P_d = P$. Besides, when the air is flowing out, it holds $P_u = P$ and $P_d = P_{atm}$. Thus, it results in

$$\psi = \begin{cases} \psi(P_s, P), & \text{if} \quad A_v \geq 0 \\ \psi(P, P_{atm}), & \text{if} \quad A_v < 0 \end{cases} \qquad (14)$$

$$\dot{m} = A_v\psi \qquad (15)$$

where A_v is equal to the open area of valve port. The model parameters for pneumatic muscle produced by FESTO Company with 400 mm length and other parts are presented in Table 1.

Table 1　Actual system parameters

Parameters	Value
M	5 kg
P_s	6 bar
n	1.06
γ	1.4
R	0.287 kJ/kgK
T	295 K
P_{atm}	1.01 bar
C_f	0.294
C_r	0.528
L_0	0.4 m
b	0.483 m
n	1.25

For evaluating this model, the mathematical based open loop test system and the experimental model (Fig. 2) have been provided where the understudy mathematical model has been adapted based on the system physical model. The flow control valve, Festo MPYE-1/8 type is used to control the inlet flow of the muscle. In order to measure the changes in muscle length due to the air pressure, Opkon′s potentiometer transducer has been applied with an accuracy of 0.01 mm. The sensor data and command signal are transferred to the PC through a data acquisition card. The wika-eco-1 pressure sensor, its output is 4-20 mA, is employed to measure the inlet air pressure of the PAM. To convert the output current of this sensor to voltage, a 250 Ω resistance should be inserted into the terminal of the data acquisition card. The PAM manufactured by Festo Company with DMSP40 part number and 400 mm length has been chosen for modeling purposes.
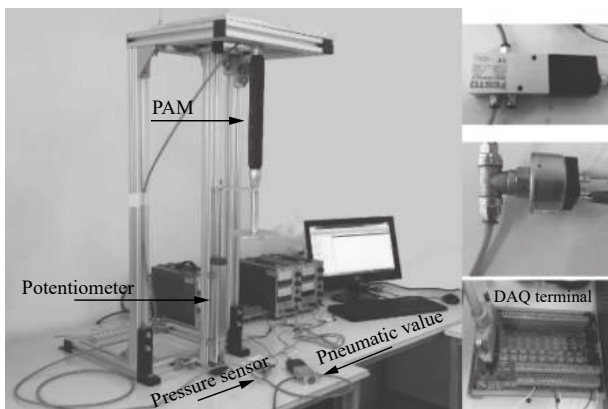
Fig. 2　Experimental setup

The most prominent processes in this regard are those that consider the saturation block to exclude the additional and irrational inputs to the system. Following that, the eliminated gravitational acceleration from the relationship, when obtaining the third derivative of the position, must be exerted. Hence, when the integration is done from the third derivative of the position, the gravitational acceleration should be added as the integral constant. Furthermore, assuming that the muscle-free status is zero, the reference signal should not exert a negative value. Comparison of the mathematical model output and experimental test output are shown in Fig. 3.
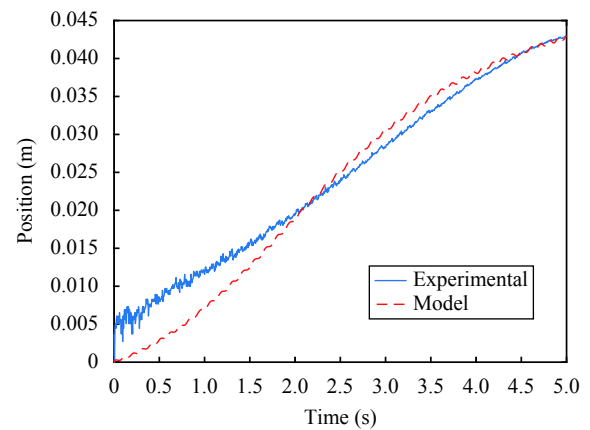
Fig. 3　Comparison of mathematical model and experimental setup output

3 Dynamic neural network

ANNs are conventionally known as both the static and dynamic. A static-algebraic relation is set for relation between the inputs and outputs of the static neural networks. However, a dynamic relation between ANN inputs and outputs appears due to its dynamic nature[26]. In the static neural networks, the network output in a defined sample encompasses some weight functions, biases and inputs and is not dependent on the input-output sets of the network in other samples, i.e., the learning capability of such networks toward the dynamic systems is merely owing to their learning approaches. Furthermore, an approach is applied for providing a dynamic relation in DNN structure[24].

In this paper, position control of a PAM has been carried out using DNN with delay lines. Delayed values of the data are employed as inputs of the network. The schematic structure of the DNN is depicted in Fig. 4.

$$y = f\left(u\left(t\right), u\left(t-1\right), \cdots, y\left(t-1\right), \cdots, y(t-n)\right). \quad (16)$$

According to the above DNN structure, the reference value at sample k and the position and actuator input at sample $k-1$ and $k-2$ are as the network inputs. The network output is the actuator input for reference tracking at sample k. Choosing former samples for the net-
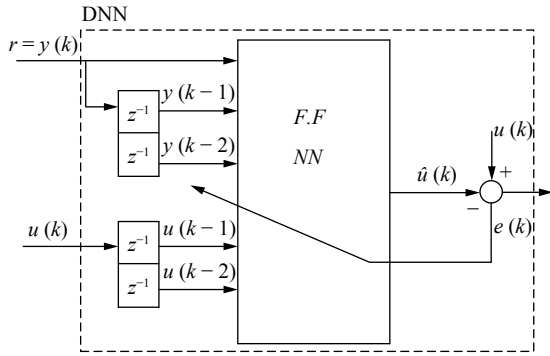
Fig. 4   DNN structure which used for position control of the PAM in this research

work input is based on the efficiency of the training. In this study, it is considered to be 2 samples. The network measured output of the introduced DNN can be given as 17 that presents the dynamic nature of the network.

$$\hat{u}(t) = f(u(t-1), u(t-2), r(t), y(t-1), y(t-2)). \quad (17)$$

As the rule for the weights of the DNN to be updated, w_{ji}^{L} can be applied for the weights of j-th neuron in L-th layer and i-th neuron in the $(L–1)$-th layer. The updating equations for the w_{ji}^{3} and w_{ji}^{2} are given as follows[26]:

$$\begin{cases} w_{ji}^{3}(n+1) = w_{ji}^{3}(n) + \Delta w_{ji}^{3}(n) \\ \Delta w_{ji}^{3}(n) = \eta \delta_{j}^{3}(n) O_{i}^{2}(n) \\ \delta_{j}^{3}(n) = O_{j}^{3}(n) \left(1 - O_{j}^{3}(n)\right) \left(T_{j}(n) - O_{j}^{3}(n)\right) \end{cases} \quad (18)$$

$$\begin{cases} w_{ik}^{2}(n+1) = w_{ik}^{2}(n) + \Delta w_{ik}^{2}(n) \\ \Delta w_{ik}^{2}(n) = \eta \delta_{j}^{2}(n) O_{k}^{1}(n) \\ \delta_{j}^{2}(n) = O_{j}^{2}(n) \left(1 - O_{i}^{2}(n)\right) \left(\displaystyle\sum_{m=1}^{N^{3}} \delta_{m}^{3}(n) w_{mi}^{3}(n)\right). \end{cases} \quad (19)$$

In the first layer, the output of the p-th neuron is attained as

$$O_{p}^{1}(n) = \sum_{l=1}^{2} w_{pl}^{1}(n) u(t-1) + \sum_{h=1}^{2} w_{ph}^{1}(n) y(t-h) + w_{p}^{1}(n) r(t) \quad (20)$$

where u, r and y indicate the chosen valve voltage, the reference signal and the PAM position, respectively[23]. It should be noted that the stability of the DNN is proved by Narendra and Parthasarathy[27].

4 Hybrid dynamic neural network

In this section, a PID controller is combined with the DNN controller to improve its performance in the presence of unexpected conditions and in lack of appropriate

and rich data. The proposed hybrid PID-DNN not only overcomes the drawbacks of the DNN controller such as inadequate performance and feeble tracking, but also discloses the substantial precise results. The control command has been provided for the actuator in accordance to the process knowledge, which is learned via the network in the training process. Hence, the PID-DNN has tracked the reference signal well, unlike the debilitated performance of the PID in the initial operation. Consequently, PID-DNN has enormous advantages such as small value of error criteria, robustness in the presence of noise, external disturbances and parametric uncertainty, a small gain of the PID controller for implementation purposes, and the most outstanding, proper performance of the controller in the temporary procedure. Fig. 5 shows the structure of the suggested hybrid controller. It should be noted that for obtaining the optimal parameters of the controller, integral time absolute error is chosen as a cost function and then, is minimized using the PSO algorithm. The integral time absolute error (ITAE) performance index has the advantages of producing smaller overshoots and oscillations than the integral of the absolute error (IAE) or the integral square error (ISE) performance indices. In addition, it is the most sensitive of the three, i.e., it has the best selectivity. The integral time-square error (ITSE) index is somewhat less sensitive and is not comfortable computationally[28]. The PSO algorithm and its procedure have been described by Falehi[29] and Lin et. al[30]. PSO as an exceptional optimization, has been developed by Kennedy and Eberhart[31, 32]. The optimal PID parameters obtained by the algorithm are reported in Table 2. The PSO convergence trend is depicted in Fig. 6.
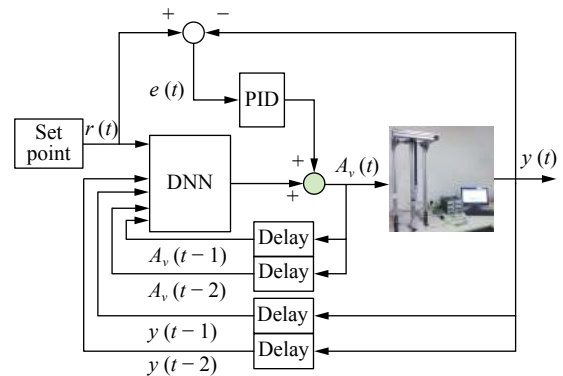
Fig. 5   Structure of the suggested hybrid controller

Table 2   Optimal PID parameters for hybrid PID-DNN controller

Parameter	Value
P	6.490
I	5.653
D	0.2146
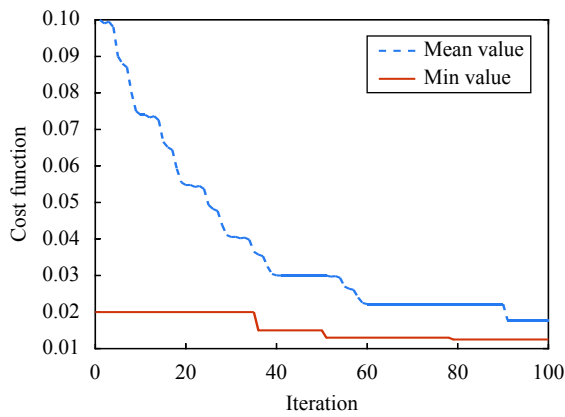
Fig. 6   PSO convergence trend

5   Simulation results

5.1   DNN training

To aggregate sufficient output data for training the neural network, some sinusoidal and step inputs with different frequencies are applied. In the experimental setup based model used for this study, all system constraints have been considered in data generation and training process. It is presumed that the input signal value is around 0.5 V for exciting the system. The input signal of data generation is represented by (21) in which a_i, b_i and f_i, $i = 1, \cdots, 4$ stand for magnitude, biases and frequencies of sinusoidal waves, respectively. Table 3 gives values of the mentioned parameters.

$$u(t) = a_4((a_1\sin(2\pi f_1 t) + b_1) + (a_2\sin(2\pi f_2 t) + b_2) + (a_3\sin(2\pi f_3 t) + b_3)) + b_4. \tag{21}$$

Table 3   Considered parameters for the input signal

Parameter	Value	Parameter	Value	Parameter	Value
a_1	10.5	f_1	2	b_1	9
a_2	9.1	f_2	5	b_2	9
a_3	9.5	f_3	20	b_3	9
a_4	3.33×10^{-8}	–	–	b_4	0.5

The input/output signal is shown in Fig. 7.

The DNN is trained using the training data and a supervised learning method. The structure of the DNN can be stated as 5-7-1, which means that the network has five input signals, seven neurons in the hidden layer and one neuron in the output layer. In order to increase the real-time implementation capability of the neural network, a two-layer neural network is used as the controller. It should be noted that a complex structure of a neural network with more layers may lead to greater performance[23]. After 10 000 epochs, the maximal error is obtained as 5.4788×10^{-5} and also, error variance is equaled to
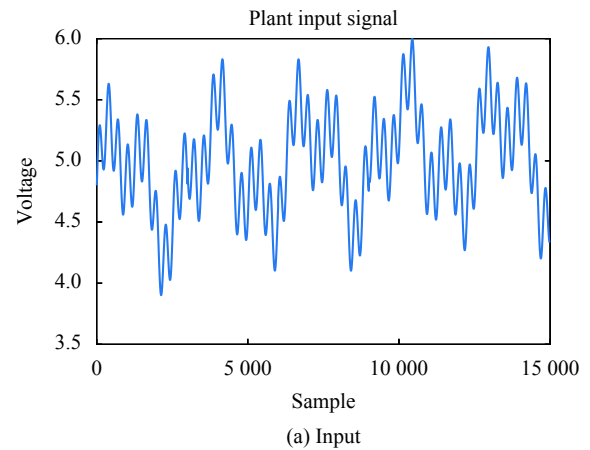
(a) Input
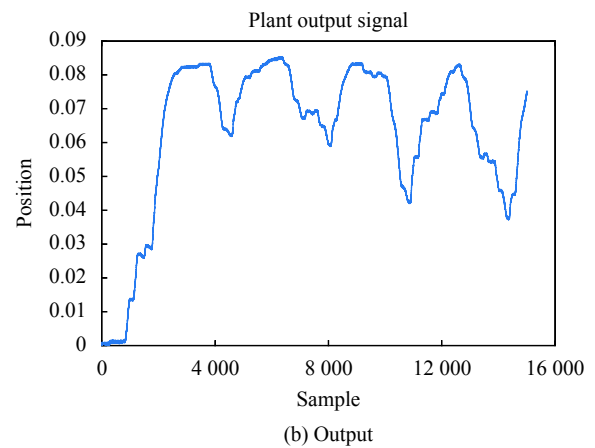
(b) Output

Fig. 7   Input/output signals extracted through the experimental setup to train the DNN

1.9998×10^{-6}. The convergence of weights and biases is depicted in Fig. 8.

5.2   Controller simulation results

In the following, the result of the hybrid PID-DNNs is presented and compared by applying the sinusoidal and trapezoidal inputs. Reference signals are determined with the viewpoint of the future aim of this study, which involves the control of pneumatic artificial muscle for using in isokinetic rehabilitation movements.

In the previous studies, however, a percentage of the muscle displacement range has been merely controlled. This problem stems from the fact that all the proposed models have substantial simplifications, e.g., eliminating the effect of the thickness of the membrane or discarding the friction between the membrane and its metal mesh. This simplification certainly reduces the accuracy of the model and then decreases the tracking performance of the model-based controller. On the other hand, utilization of advanced system identification approaches such as the neural network have the ability to identify the system behavior, regardless of the model simplifications, uncertainties, time-varying, and unmodified dynamics. Thus, the
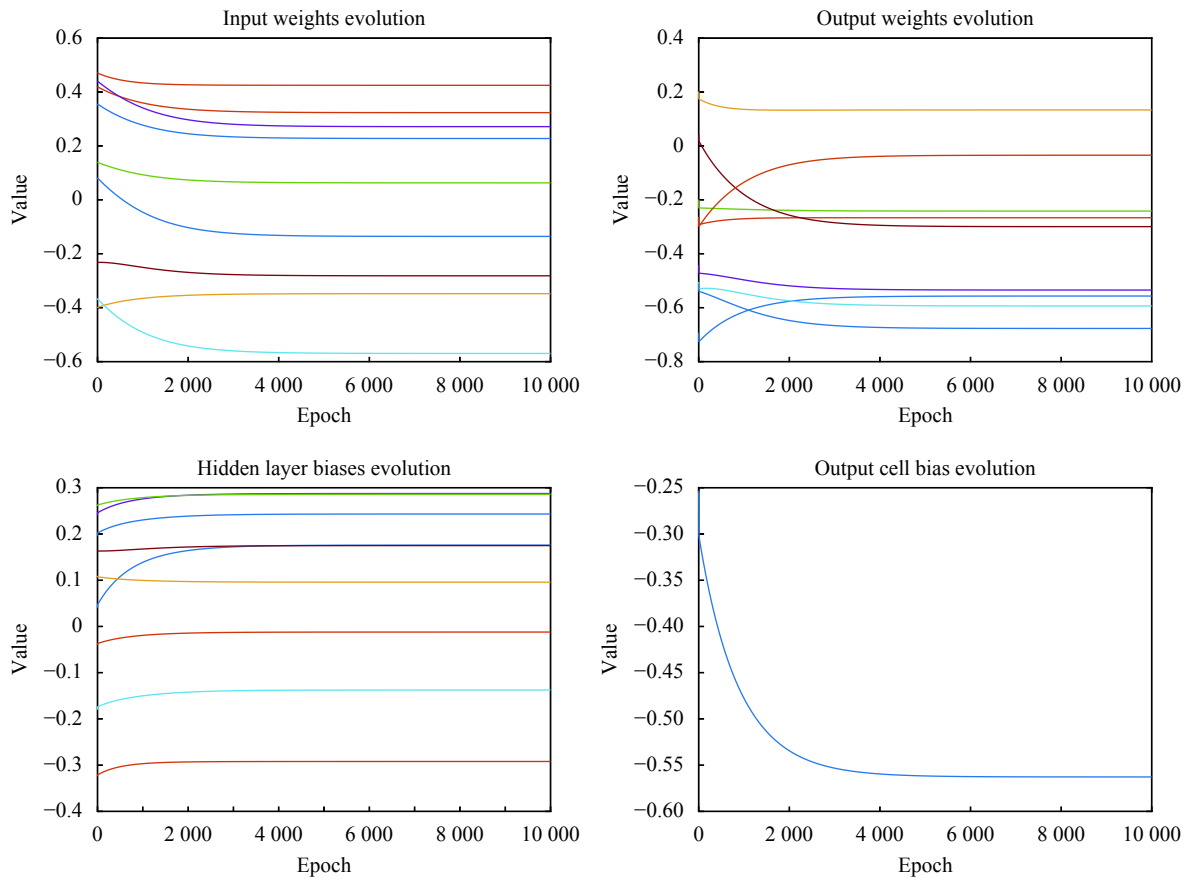
Fig. 8 Convergence of weights and biases (Color versions of the figures in this paper are available online)

trained neural network by using an input-output data, which include the entire course, can act in the same way as it controls and delivers the desired results. Despite the previous studies, inputs are somehow selected to assert the ability of controller throughout the entire course of the muscle. It is worth mentioning that the simulations have been performed by inserting a parametric uncertainty in the mass of the attached muscle.

To study the control signal, the opening of the valve spool is considered as the controller output. The maximum value for this variable can be $6.28\,\mathrm{mm}^2$. Therefore, a saturated block with the maximum value for the valve command is considered to complete accordance of simulation with the actual system.

Figs. 9–10 shows the result of the position tracking of the trapezoidal and sinusoidal signals in simulation respectively. Fig. 11 represents the tracking error of the reference signals.

As can be seen from Figs. 9–11, the suggested controller has presented an effective performance in tracking the reference signals throughout the displacement range of the muscle. The tracking errors in the entire course of the PAM for sinusoidal and trapezoidal reference signals were about 2.3% and 5.1%, respectively.

Fig. 12 represents the controller output for the both reference signals.
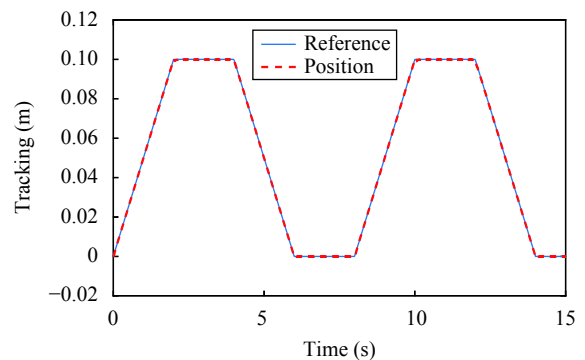
Fig. 9 Trapezoidal signal tracking in simulation
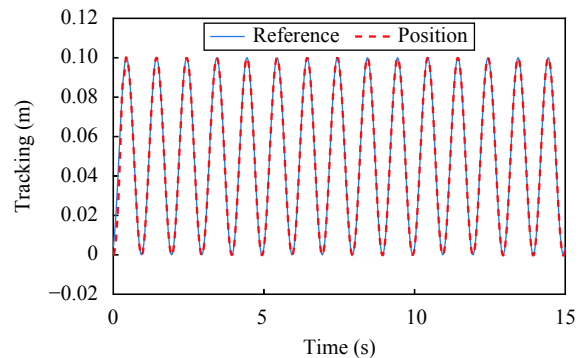
Fig. 10 Sinusoidal signal tracking in simulation
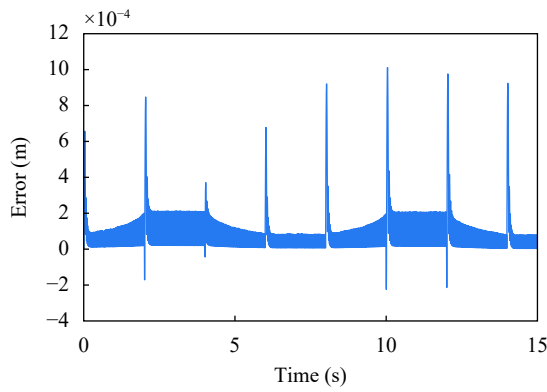
(a) Trapezoidal
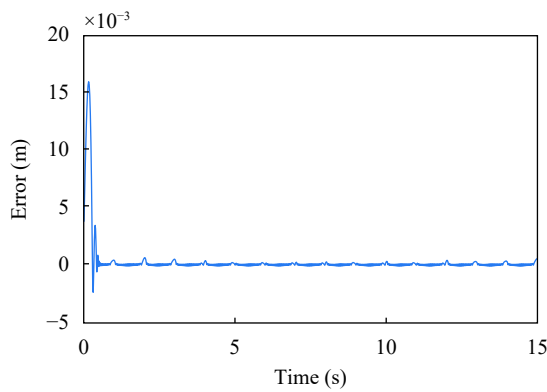
(b) Sinusoidal

Fig. 11   Tracking errors
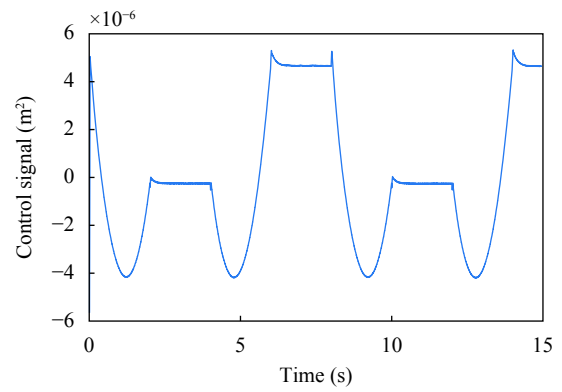
(a) Trapezoidal
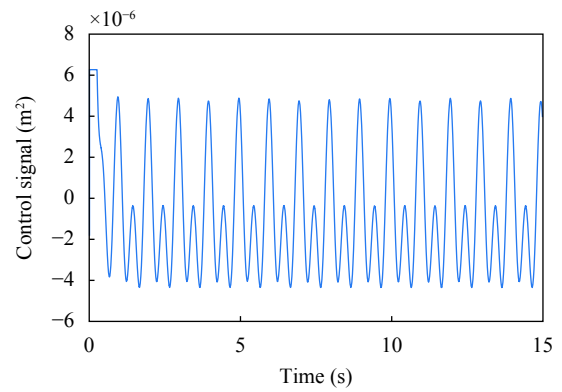
(b) Sinusoidal

Fig. 12   Control signals

According to Fig. 12, the controller output fluctuated only in small intervals and at a fast switching of the derivative of the reference signal. Another point in exploring the control signal is its sign. In the valve model, the positive value is defined for one port and the negative value is defined for another port. The zero value will result in two port closure.

To indicate the priority of the proposed PID-DNN controller, integral error criteria are considered for comparing the result of the proposed controller with conventional sliding mode control (SMC) and optimal PID. The obtained error criteria are shown in Table 4. According to Table 4, the values of these criteria for the controller indicates the accuracy of the proposed controller.

$$ITAE = \int t \left| e\left(t \right) \right| \mathrm{d}t$$

$$ISE = \int \left(e\left(t \right) \right)^2 \mathrm{d}t$$

$$IAE = \int \left| e\left(t \right) \right| \mathrm{d}t. \tag{22}$$

6   Experimental results and discussion

In this section, the performance of the proposed controller is evaluated through the experimental test. In this

Table 4   Error criteria for proposed controller

Criteria	PID-DNN	SMC	Optimal PID
ITAE	0.01158	0.8926	0.9744
ISE	8.1803×10^{-2}	0.5619	0.8792
IAE	1.615×10^{-3}	0.7108	0.9601

regard, the control command is applied to the pneumatic valve via a data acquisition card (DAQ). The final position of the PAM, which moves a mounted weight, is measured by a linear potentiometer and its value is returned using a DAQ card. A schematic of the experimental setup is shown in Fig. 2. Two signals (sinusoidal and trapezoidal) are considered as reference trajectories. Fig. 13 shows the performance of the controller in tracking the sinusoidal trajectory.

The experimental test of the controller with a sinusoidal trajectory is shown in Fig. 13. Deviation from the reference signal at the bottom and top of the sinusoidal signal peaks results in the reduction of the controller precision with respect to the simulation, which may have many reasons. One reason can be changing the dynamics and increasing uncertainties in the PAM model at the beginning and end of the range. Indeed, the effect of this factor has been minimized in the proposed method due to
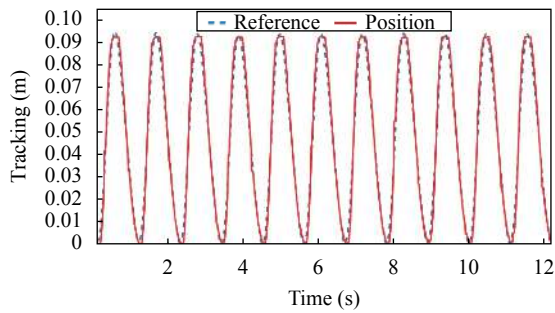
Fig. 13   Sinusoidal signal tracking in experimental test

the optimizations and accuracy of the trained NN. In applying the control signal to the pneumatic valve, the effect of the dead band has been minimized by applying a compensator function. Another reason may be hardware issues and inadequacies of laboratory equipment, such as the presence of a stiction in the pneumatic valve or a clearance in the connection between the pneumatic muscle and linear potentiometer. By examining how the controller performs in tracking the trapezoidal signal, a better understanding of the issues can be found. Fig. 14 shows the performance of the controller in tracking the trapezoidal signal.
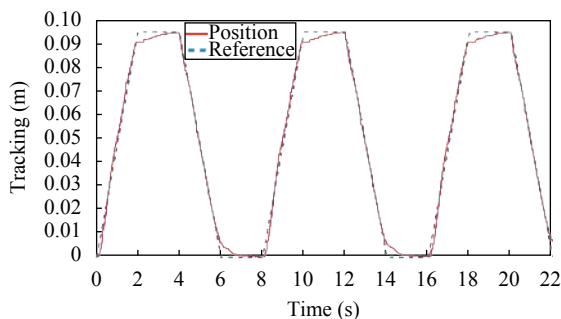
Fig. 14   Trapezoidal signal tracking in experimental test

According to Fig. 14, tracking performance of the trapezoidal signal exclusively in up and down of range has a deviation. Fig. 14 also shows that the muscle′s settling time is 1.4 s. In the areas where the spool of the valve has to be changed and air pressure is transferred from one port to another port, the performance of the valve is favorable indicating the suitable performance of the dead-band compensation function. On the other hand, there is no delay in tracking the inclined lines of the reference signal. Due to the deviation and chattering at the beginning and end of the course, it can be concluded that the trained neural network for small displacement of the PAM is less accurate than the rest of its course. The model and structure of the muscle cylinder at the end of its displacement range have been modified from the full cylinder shape, and beginning and end of its membrane are inclined leading to a decrease in the accuracy of reference signal tracking. Nevertheless, due to the intelligence

of the proposed method and the efforts made to cover the entire course of the PAM, all the inaccuracies are only led to a reduction in the system settling time. The drawbacks and hardware issues in addition to creating small chattering in the middle of the movement range intensify relative decline in the accuracy of the controller performance at the beginning and end of the PAM course.

Overall, the performance of the controller was identified as satisfactory for tracking various reference signals and the results were within an acceptable range with an estimated error of less than 5.1%. This means that the proposed controller can be used for the control system of an isokinetic rehabilitation robot.

7 Conclusions

In this paper, a hybrid PID-dynamic neural network (PID-DNN) controller is proposed to accurately control the pneumatic artificial muscle (PAM) position. Particle swam optimization is applied to optimally tune the parameters of the suggested controller. On the other hand, the understudy model is an experimental model on which all the physical elements are considered. Three criteria as objective functions are used to evaluate the performance of the proposed controller. Furthermore, to confirm the tracking performance of the hybrid controller in controlling the PAM, it has been implemented on a test bench. Experimental tests and simulation results show the outstanding performance of the PID-DNN controller in tracking the reference signals in the entire displacement range of the PAM. Also, it can be seen that the trained neural network for small displacement of the PAM is less accurate than the rest of its course. However, the highest achieved accuracy in tracking the reference signals was calculated as 2.3% of error for the sinusoidal signal and 5.1% for the trapezoidal signal.

References

[1] S. Liu, J. E. Bobrow. An analysis of a pneumatic servo system and its application to a computer-controlled robot. *Journal of Dynamic Systems, Measurement, and Control*, vol. 110, no. 3, pp. 228–235, 1988. DOI: 10.1115/1.3152676.

[2] J. Y. Lai, C. H. Menq, R. Singh. Accurate position control of a pneumatic actuator. *Journal of Dynamic Systems, Measurement, and Control*, vol. 112, no. 4, pp. 734–739, 1990. DOI: 10.1115/1.2896202.

[3] B. W. McDonell, J. E. Bobrow. Adaptive tracking control of an air powered robot actuator. *Journal of Dynamic Systems, Measurement, and Control*, vol. 115, no. 3, pp. 427–433, 1993. DOI: 10.1115/1.2899119.

[4] D. G. Caldwell, G. A. Medrano-Cerda, M. Goodwin. Control of pneumatic muscle actuators. *IEEE Control Systems Magazine*, vol. 15, no. 1, pp. 40–48, 1995. DOI: 10.1109/37.341863.

[5] D. G. Caldwell, G. A. Medrano-Cerda, M. J. Goodwin. Braided pneumatic actuator control of a multi-jointed manipulator. In *Proceedings of IEEE Systems Man and Cy-*

bernetics Conference, IEEE, Le Touquet, France, vol. 1, pp. 423–428, 1993. DOI: 10.1109/ICSMC.1993.384780.

[6] J. Schröder, K. Kawamura, T. Gockel, R. Dillmann. Improved control of a humanoid arm driven by pneumatic actuators. In *Proceedings of Humanoids 2003*, IEEE, Karlsruhe, Germany, 2003.

[7] S. V. Krichel, O. Sawodny, A. Hildebrandt. Tracking control of a pneumatic muscle actuator using one servovalve. In *Proceedings of American Control Conference*, IEEE, Baltimore, USA, pp. 4385–4390, 2010. DOI: 10.1109/ACC.2010.5530767.

[8] X. R. Shen. Nonlinear model-based control of pneumatic artificial muscle servo systems. *Control Engineering Practice*, vol. 18, no. 3, pp. 311–317, 2010. DOI: 10.1016/j.conengprac.2009.11.010.

[9] N. Zamani Meymian, N. N. Clark, T. Musho, M. Darzi, D. Johnson, P. Famouri. An optimization method for flexural bearing design for high-stroke high-frequency applications. *Cryogenics*, vol. 95, pp. 82–94, 2018. DOI: 10.1016/j.cryogenics.2018.09.008.

[10] A. Yazdizadeh, K. Khorasani. Adaptive time delay neural network structures for nonlinear system identification. *Neurocomputing*, vol. 47, no. 1–4, pp. 207–240, 2002. DOI: 10.1016/S0925-2312(01)00589-6.

[11] K. X. Xing, Y. J. Wang, Q. M. Zhu, H. Y. Zhou. Modeling and control of McKibben artificial muscle enhanced with echo state networks. *Control Engineering Practice*, vol. 20, no. 5, pp. 477–488, 2012. DOI: 10.1016/j.conengprac.2012.01.002.

[12] K. K. Ahn, H. P. H. Anh. A new approach for modelling and identification of the pneumatic artificial muscle manipulator based on recurrent neural networks. *Proceedings of the Institution of Mechanical Engineers, Part I: Journal of Systems and Control Engineering*, vol. 221, no. 8, pp. 1101–1121, 2007. DOI: 10.1243/09596518JSCE432.

[13] K. K. Ahn, H. P. H. Anh. Design and implementation of an adaptive recurrent neural networks (ARNN) controller of the pneumatic artificial muscle (PAM) manipulator. *Mechatronics*, vol. 19, no. 6, pp. 816–828, 2009. DOI: 10.1016/j.mechatronics.2009.04.006.

[14] N. N. Son, C. Van Kien, H. P. H. Anh. A novel adaptive feed-forward-PID controller of a SCARA parallel robot using pneumatic artificial muscle actuator based on neural network and modified differential evolution algorithm. *Robotics and Autonomous Systems*, vol. 96, pp. 65–80, 2017. DOI: 10.1016/j.robot.2017.06.012.

[15] J. Z. Fan, J. Zhong, J. Zhao, Y. H. Zhu. BP neural network tuned PID controller for position tracking of a pneumatic artificial muscle. *Technology and Health Care*, vol. 23, no. S2, pp. S231–S238, 2015. DOI: 10.3233/THC-150958.

[16] H. P. H. Anh. Online tuning gain scheduling MIMO neural PID control of the 2-axes pneumatic artificial muscle (PAM) robot arm. *Expert Systems with Applications*, vol. 37, no. 9, pp. 6547–6560, 2010. DOI: 10.1016/j.eswa.2010.02.131.

[17] L. D. Khoa, D. Q. Truong, K. K. Ahn. Synchronization controller for a 3-R planar parallel pneumatic artificial muscle (PAM) robot using modified ANFIS algorithm. *Mechatronics*, vol. 23, no. 4, pp. 462–479, 2013. DOI: 10.1016/j.mechatronics.2013.03.011.

[18] X. Z. Jiang, Z. H. Wang, C. Zhang, L. L. Yang. Fuzzy neural network control of the rehabilitation robotic arm driven by pneumatic muscles. *Industrial Robot*, vol. 42, no. 1, pp. 36–43, 2015. DOI: 10.1108/IR-07-2014-0374.

[19] Y. T. Wang, R. H. Wong, J. T. Lu. Comparative studies of the set up of two-dimensional pneumatic arm systems by muscle and rotational actuators. *Proceedings of the Institution of Mechanical Engineers, Part I: Journal of Systems and Control Engineering*, vol. 221, no. 5, pp. 743–748, 2007. DOI: 10.1243/09596518JSCE413.

[20] Y. Cao, J. Huang, G. Z. Ding, Y. J. Wang. Design of nonlinear predictive control for pneumatic muscle actuator based on echo state Gaussian process. *IFAC-PapersOnLine*, vol. 50, no. 1, pp. 1952–1957, 2017. DOI: 10.1016/j.ifacol.2017.08.390.

[21] C. J. Chiang, Y. C. Chen. Neural network fuzzy sliding mode control of pneumatic muscle actuators. *Engineering Applications of Artificial Intelligence*, vol. 65, pp. 68–86, 2017. DOI: 10.1016/j.engappai.2017.06.021.

[22] G. Das, P. K. Pattnaik, S. K. Padhy. Artificial neural network trained by particle swarm optimization for non-linear channel equalization. *Expert Systems with Applications*, vol. 41, no. 7, pp. 3491–3496, 2014. DOI: 10.1016/j.eswa.2013.10.053.

[23] M. Mazare, M. Taghizadeh, M. G. Kazemi. Optimal hybrid scheme of dynamic neural network and PID controller based on harmony search algorithm to control a PWM-driven pneumatic actuator position. *Journal of Vibration and Control*, vol. 24, no. 16, pp. 3538–3554, 2018. DOI: 10.1177/1077546317707102.

[24] D. H. Zhang, X. G. Zhao, J. D. Han. Active model-based control for pneumatic artificial muscle. *IEEE Transactions on Industrial Electronics*, vol. 64, no. 2, pp. 1686–1695, 2017. DOI: 10.1109/TIE.2016.2606080.

[25] L. J. Zhu, X. Y. Shi, Z. Y. Chen, H. T. Zhang, C. H. Xiong. Adaptive servomechanism of pneumatic muscle actuators with uncertainties. *IEEE Transactions on Industrial Electronics*, vol. 64, no. 4, pp. 3329–3337, 2017. DOI: 10.1109/TIE.2016.2573266.

[26] C. P. Chou, B. Hannaford. Static and dynamic characteristics of McKibben pneumatic artificial muscles. In *Proceedings of IEEE International Conference on Robotics and Automation*, IEEE, San Diego, USA, 1994. DOI: 10.1109/ROBOT.1994.350977.

[27] K. S. Narendra, K. Parthasarathy. Identification and control of dynamical systems using neural networks. *IEEE Transactions on Neural Networks*, vol. 1, no. 1, pp. 4–27, 1990. DOI: 10.1109/72.80202.

[28] D. Maiti, A. Acharya, M. Chakraborty, A. Konar, R. Janarthanan. Tuning PID and PI/λ D δ controllers using the integral time absolute error criterion. In *Proceedings of the 4th International Conference on Information and Automation for Sustainability*, IEEE, Colombo, Sri Lanka, pp. 457–462, 2008. DOI: 10.1109/ICIAFS.2008.4783932.

[29] A. D. Falehi. Optimal design of fuzzy-AGC based on PSO & RCGA to improve dynamic stability of interconnected multi area power systems. *International Journal of Automation and Computing*, to be published. DOI: 10.1007/s11633-017-1064-0.

[30] G. H. Lin, J. Zhang, Z. H. Liu. Hybrid particle swarm optimization with differential evolution for numerical and engineering optimization. *International Journal of Automation and Computing*, vol. 15, no. 1, pp. 103–114, 2018. DOI: 10.1007/s11633-016-0990-6.

[31] J. Kennedy. Particle swarm optimization. In *Proceedings of the Encyclopedia of Machine Learning*, Springer, Boston, USA, pp. 760–766, 2011.

[32] J. Kennedy, R. C. Eberhart. A discrete binary version of the particle swarm algorithm. In *Proceedings of IEEE International Conference on Systems, Man, and Cybernetics. Computational Cybernetics and Simulation*, IEEE, Orlando, USA, vol. 5, pp. 4104–4108, 1997. DOI: 10.1109/ICSMC.1997.637339.

Mahdi Chavoshian received the B. Sc. degree in mechanical engineering from Shahrood University of Technology, Iran in 2008, and the M. Sc. degree in mechanical engineering from Islamic Azad University South Tehran Branch, Iran in 2011. Currently, he is a Ph. D. degree candidate in mechanical engineering at Department of Mechanical and Energy Engineering, Shahid Beheshti University, Iran.

His research interests include dynamic systems, feedback control systems, specially modeling and control of servo pneumatic systems.

E-mail: m_Chavoshian@sbu.ac.ir

ORCID iD: 0000-0002-4389-1451

Mostafa Taghizadeh received the B. Sc. and M. Sc. degrees in mechanical engineering from the University of Tehran, Iran in 1995 and 1997, respectively, and the Ph. D. degree in mechanical engineering from K. N. Toosi University of Technology, Iran in 2008. In 2008, he was a faculty member at Power and Water University of Technology, Iran. Currently, he is an assistant professor at Department of Mechanical and Energy Engineering, Shahid Beheshti University, Iran. He has published about 35 refereed journal and conference papers.

His research interests include fluid power control systems, robotics and feedback control systems

E-mail: mo_taghizadeh@sbu.ac.ir (Corresponding author)
ORCID iD: 0000-0003-2295-8132

Mahmood Mazare received the M. Sc. degree in mechanical engineering from Shahid Beheshti University, Iran in 2016. Currently, he is a member of control and robotics laboratory at Department of Mechanical and Energy Engineering, Shahid Beheshti University, Iran.

His research interests include control, robotics, and dynamic systems.

E-mail: m_mazare@sbu.ac.ir

Articles may interest you